Design and Implementation of a Compact Super-Wideband Printed Antipodal Antenna Using Fractal Elements

A. Dastranj
Department of Electrical Engineering, Faculty of Engineering, Yasouj University, Yasouj, Iran, dastranj@yu.ac.ir
Corresponding author: dastranj@yu.ac.ir

***Abstract*- A compact printed fractal antipodal bow-tie antenna is designed and implemented to simultaneously cover the operations in the C, X, and Ku-bands. It is demonstrated that by addition of small fractal elements at the sides of hexagonal arms of the bow-tie, a wide operating frequency range of 3.3 to 19.1 GHz can be covered while antenna size is only 30×34×1.2 mm^3. In order to match the antenna to the 50Ù SMA connector, a multi-section microstrip line of different widths is designed. The simulation results obtained from HFSS simulator package are verified by experimental measurements. Measured data are in good agreement with the simulated results. The frequency- and time-domain characteristics of the antenna including impedance matching, far-field patterns, radiation efficiency, gain, and fidelity factor are presented and discussed. The proposed antenna features 141% impedance bandwidth (defined by -10-dB reflection coefficient), small size, and desirable radiation patterns that make it excellent candidate for integration in broadband array systems.**

***Index Terms*-** *Fractal elements, hexagonal radiators, printed fractal antipodal bow-tie antenna (PFABTA), super-wideband*

I. INTRODUCTION

Printed fractal antennas can be used in variety of applications, especially where space is limited. These antennas have shown the possibility to miniaturize antenna systems and to improve input impedance matching [1, 2]. Also, a fractal antenna can be designed to operate over a wide range of frequencies using the self-similarity properties associated with fractal geometry structures [3-6]. An example of exploiting the benefits of fractals in antenna systems is phased arrays, where fractals can reduce mutual coupling and allow for lower scan angles.

Notice that communication and phased array systems that operate in the C, X, and Ku-bands are usually designed using separate antennas for each band. Since it is becoming more and more important to use such systems in one setting, it is desirable to design a single antenna that operates in three frequency bands. This, in turn, requires a wideband antenna that covers the three bands. In addition, phas

Manuscript received 19-Jan.-2018 and revised 15-April-2018,
Accepted on 3-May-2018
P- ISSN: 2322-4088
E- ISSN: 2322-3936

ed array systems require compact radiating elements with end fire patterns. An interesting way to sfy the aforementioned requirements has been the use of fractal end-fire bow-tie antenna which has come a recent topic of interest.

Different fractal antennas such as Minkowski loop [7], Koch curve monopole [8], Koch island h [9], Sierpinski carpet [10, 11] and Sierpinski gasket [12, 13] have been designed by using self-arity and space-filling concepts of fractals to achieve wideband characteristics. Also, many s have been used to reduce the size and enhance the bandwidth of printed bow-tie antennas [14-27]. A triband coplanar waveguide (CPW)-fed printed bow-tie slot antenna was presented in [14]. In [15], wo different flexible bow-tie antennas with reduced metallization based on the phenomenon that the ajority of the current density was confined towards the edges of the patch were reported. After the ters of the triangular parts were removed, the performance of antenna did not have significant on. A low-profile bow-tie antenna with multiband operation was presented for multistandard wireless communication applications [16]. In order to provide multiband performance, shunt strips and series gaps with inductive and capacitive behavior, respectively, were added to the bow-tie antenna. A band Koch-like sided fractal bow-tie dipole antenna with moderate gain (3.5–7 dBi) and high cy (60%-80%) was reported in [17]. In [18], a directional wideband self-grounded bow-tie antenna ith a volume of 54×58×24 mm^3 can cover a bandwidth of 3–15 GHz. In [19], an ultra-wideband B) bow-tie quasi-self-complementary antenna (QSCA) with a compact size of 10×35 mm was printed on an FR4 dielectric substrate with 1.6 mm thickness. It consisted of two radiating elements: a horn haped conductive patch and a counterpart horn-shaped slot. A CPW-like matching technique ing a central strip and a triangular piece was used to modulate the impedance matching. The bow-tie QSCA features an impedance bandwidth of 116% from 3.04 to 11.47 GHz. In [20], a microstrip balun fed broadband printed modified bow-tie antenna, consisting of rounded T-shaped slot loaded bow ms printed on a low-loss RT/duroid 5870 substrate with a modified ground plane underneath, was posed. However, it has a large size of 43×60 mm. In [21], a directive bow-tie antenna for three-sional microwave imaging systems was designed. By adding inductive strips to the capacitive antenna element and thereby lowering the cutoff operational frequency, an impedance bandwidth of 117% 85-3.25 GHz) was achieved. A new bow-tie slot antenna was implemented in [22]. By replacing a ventional narrow rectangular slot with a bow-tie shaped slot, unidirectional radiation characteristics over a bandwidth of 1.03 GHz (9.4%) were obtained. In [23], a CPW-fed bow-tie slot antenna with a dual-band function was presented. It can provide two operating bandwidths of 1450 MHz (about % centred at 4.43 GHz) and 3500 MHz (about 37.8% centred at 9.25 GHz). In [24], a bow-tie slot enna fed by an asymmetric coplanar waveguide (ACPW) with different slot lengths was presented. By adjusting the length of one ACPW slot, an operating frequency range from 2.76 to 8.1 GHz (for $|S_{11}| < -10$ dB) was obtained. A bow-tie antenna with frequency-reconfigurable behavior for worldwide eroperability for microwave access, Bluetooth, and wireless local area network systems was presented in [25]. It can be adjusted to cover the frequency ranges of 2.2–2.53, 2.97–3.71, or 4.51–6 GHz with

desirable radiation characteristics. In [26], by using a pair of tilted bow-tie radiators fed through substrate integrated waveguide feed-line, a millimeter-wave bow-tie antenna with an impedance bandwidth of 57□64 GHz was designed. Recently, a fractal artificial magnetic conductor structure was designed as the ground plane of a printed bow-tie antenna for gain enhancement and low profile [27]. The antenna can cover a bandwidth from 1.64 to 1.94 GHz, with a relative frequency bandwidth of 16.7%.

The objective of this article is to design a compact super-wideband antenna with simple structure and satisfactory radiation characteristics, using fractal elements. Another important issue is to keep the antenna inexpensive and easy to manufacture. To accomplish these goals, a new structure comprises of an antipodal bow-tie with hexagonal radiators is proposed. Furthermore, Small hexagon elements are added to the sides of the antenna radiators to achieve a wide operation along with a compact size. In order to match the antenna to the 50Ù SMA connector, a multi-section microstrip line of different widths is designed. The simulation results obtained from HFSS simulator package are verified by experimental measurements. The proposed printed fractal antipodal bow-tie antenna (PFABTA) with a compact size of 30×34×1.2 mm^3 can cover the C, X and Ku-bands from 3.3 to 19.1 GHz (141% impedance bandwidth defined by -10-dB reflection coefficient). Measured results show that the designed PFABTA features desirable frequency-domain characteristics such as stable radiation patterns, high radiation efficiency, and reasonable gain. Furthermore, to analyze the proposed antenna in time domain, fidelity factor is investigated. Compared to recent designs reported in [22-25], the proposed antenna features a wider bandwidth as well as a smaller size. The proposed PFABTA is a good candidate for use in broadband communication or phased array systems due to its wide operating bandwidth, light weight, low cost, low profile, and ease of fabrication.

II. FRACTAL ANTIPODAL BOW-TIE ANTENNA DESIGN

The configuration of the proposed antenna labeled with the design parameters is shown in Fig. 1. It can be seen that unlike the conventional bow-tie antennas, one of the bow-tie arms is printed on the bottom layer of the dielectric substrate and the other is printed on the top layer of the substrate. The proposed PFABTA comprises of an antipodal bow-tie with hexagonal arms which small hexagon elements are added to the sides of the antenna radiators to achieve a wideband operation along with a compact size. To match the antenna to the 50Ù SMA connector, a multi-section microstrip line of different widths is used. The antenna is printed on an FR4 substrate with permittivity of 4.4, thickness of 1.2 mm, and loss tangent of 0.02. The total size of the antenna is 30× 34×1.2 mm^3. For further insight, the proposed antenna without the fractal elements (antenna 1) and with the second repetition of the small fractal elements (antenna 2) was simulated by using electromagnetic simulator package Ansoft HFSS. Fig. 2 illustrates the configurations of antennas 1 and 2. The values of the design parameters are as follows: L=30 mm, W=34 mm, a=6mm, b=2mm, c=7mm, d=1mm, Lg=5 mm,

L1=3.6 mm, L2=10.9 mm, L3=2.2 mm, W1=2.8 mm, W2=2.6 mm, W3=1.4 mm, Wm=2.22 mm, α=112.54°, β=134.92°. The final optimized values of the design parameters are obtained through numerous simulations via Ansoft HFSS. The corresponding impedance matching curves of the designed antennas are given in Fig. 3. As shown in this figure, the proposed antenna without the fractal elements (antenna 1) covers the frequency range of 3.5 to 16 GHz (128% impedance bandwidth defined by -10-dB reflection coefficient). It is observed that after adding the small hexagon elements to the sides of the antenna radiators (proposed antenna), the lower and higher band edge frequencies are shifted from 3.5 and 16 GHz to 3.3 and 19.1 GHz, respectively, which leads to a bandwidth of about 141 %. In the next step, the second repetition of the small fractal elements are added to the antenna (antenna 2), and as depicted in Fig. 3, the impedance matching of the antenna deteriorates in 10–11 GHz frequency range. As a result, *antenna 2 covers two frequency bands of 3.2–10 GHz (103% bandwidth) and 11–18.5 GHz (50% bandwidth) for* $|S_{11}| < -10$ *dB.*

An extensive numerical sensitivity analysis was conducted to understand the effects of different geometrical parameters on the performance of the proposed antenna. Through numerous simulations, it was found that the main design parameters a and b considerably affect the antenna reflection coefficient. Fig. 4 shows the simulated reflection coefficient curves for different values of the side length a while the other geometrical parameters of the antenna are kept fixed. As shown in this figure, the reflection coefficient deteriorates within the whole band as a changes. The optimal value of this parameter for maximum impedance bandwidth is 6 mm. Fig. 5 shows the influence of the side length b on the reflection coefficient of the antenna while the other design parameters are unchanged. As it can be observed, this parameter mostly affects the antenna reflection coefficient at high frequencies. As shown in this figure, the bandwidth of the antenna enhances as the side length b increases from 1 to 2 mm. However, when b increases to 4 mm, the antenna impedance matching deteriorates at the higher frequencies of the band. Referring to Fig. 5, it is seen that selecting the optimal value of b=2 mm leads to wider impedance bandwidth.

In order to more investigate the influence of the small hexagonal fractal elements on the impedance characteristic of the proposed antenna, the surface current distribution on the antenna radiators and ground plane at 3.5 and 18 GHz is presented in Fig. 6. As shown in this figure, the current distribution on the fractal elements at 3.5 GHz has a small magnitude, while at 18 GHz current distribution is mainly concentrated on the fractal elements. This means the fractal elements affect impedance characteristic at high frequencies. It is seen that the surface current distribution of Fig. 6 is compatible with the reflection coefficient plotted in Fig. 5. Both figures indicate that high frequency behavior of the antenna can be controlled by fractal elements.

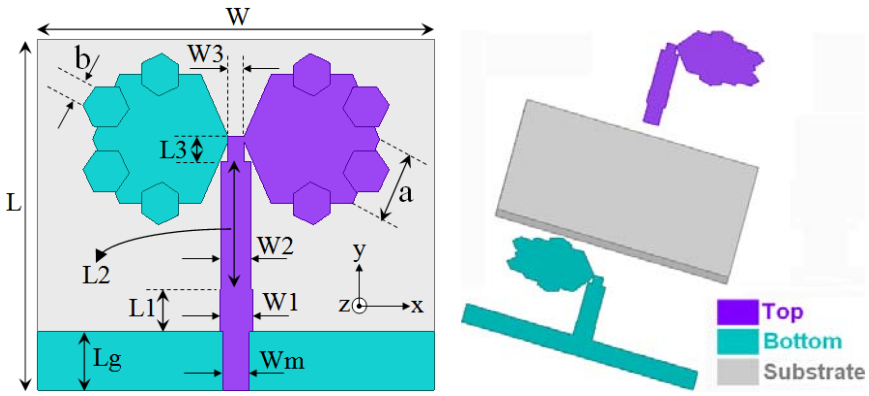

Fig. 1. Configuration *and geometrical parameters of the proposed antenna.*

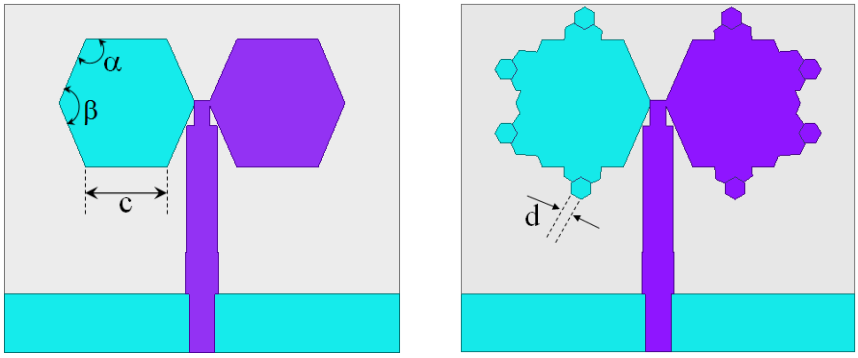

(a) *(b)*

Fig. 2. Configuration *of the proposed antenna without the fractal elements (antenna 1) and with the second* repetition of the *small fractal elements (antenna 2), (a) antenna 1, (b) antenna 2.*

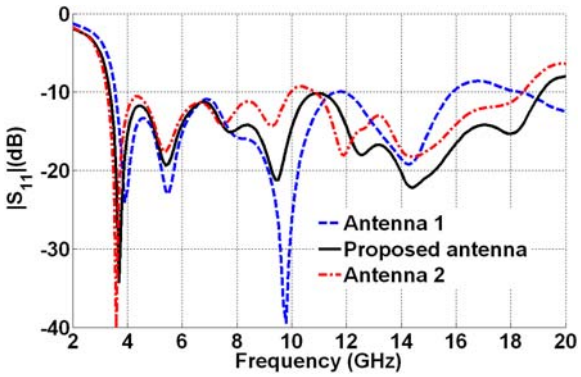

Fig. 3. Numerical reflection coefficient curves of the designed antennas.

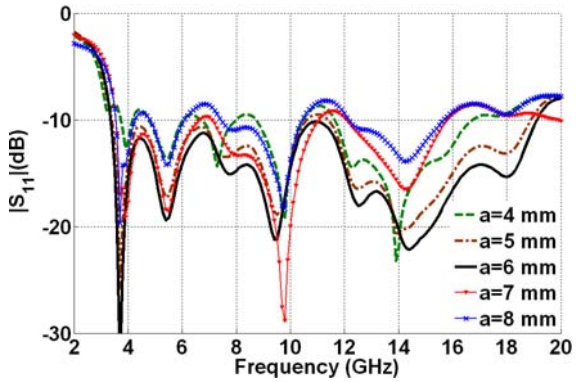

Fig. 4. Simulated reflection coefficient curves of the proposed antenna for different values of side length *a*.

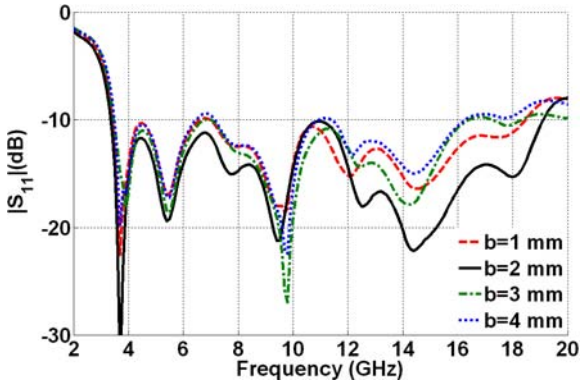

Fig. 5. Simulated reflection coefficient curves of the proposed antenna for different values of side length *b*.

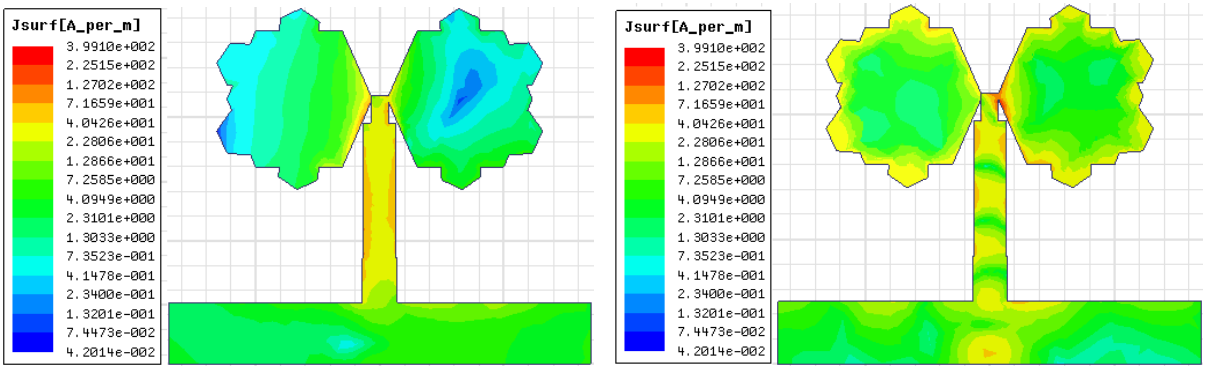

(a) *(b)*

Fig. 6. Surface current distribution of the proposed antenna at (a) 3.5 and (b) 18 GHz.

III. RESULTS AND DISCUSSION

To verify the simulation results obtained by Ansoft HFSS, the designed antennas were fabricated and tested. Fig. 7 shows the photograph of the fabricated prototypes. In this section, the experimental results are presented, discussed, and compared with the numerical results.

A. Frequency-domain results

Fig. 8 presents the comparison of experimental and numerical reflection coefficient curves of the proposed antenna, antenna 1, and antenna 2. Refereeing to Fig. 8(a), both measured and simulated results show that the proposed PFABTA can provide the impedance bandwidth of 3.3-19.1 GHz (141% bandwidth for $|S_{11}| < -10$ dB) which simultaneously covers the C (4-8 GHz), X (8-12 GHz) and Ku (12-18 GHz)-bands. Also, the experimental results of Figs. 8(b) and 8(c) show reasonable concordance with the numerical data. As shown in these figures, the bandwidth of antenna 1 (the antenna without the fractal elements) is from 3.5 to 16 GHz, and antenna 2 (the antenna with the second repetition of the fractal elements) features dual-band operation.

To determine the overall bandwidth of the antenna, other radiation characteristics such as far-field patterns, gain, and efficiency must also be carefully examined over the entire frequency band. The

far-field radiation patterns of the proposed PFABTA were measured at different frequencies. For brevity,

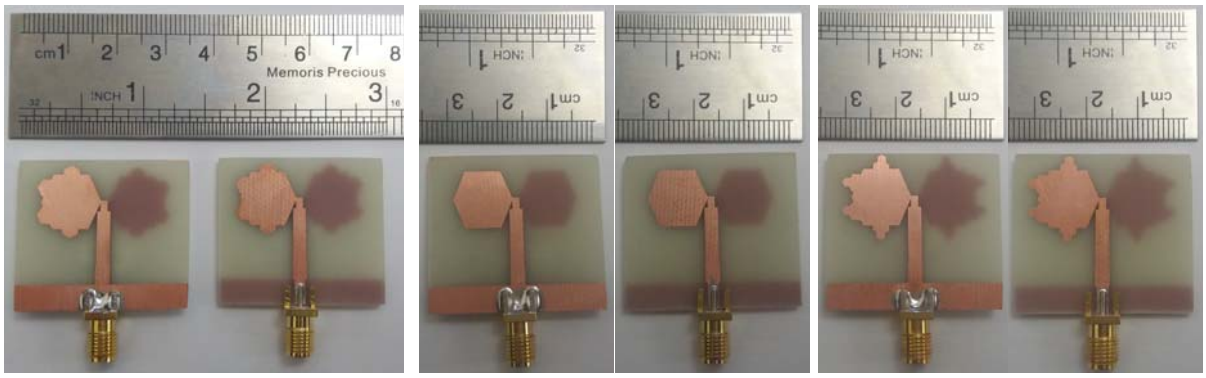

(a) *(b)* *(c)*

Fig. 7. Photographs of the fabricated prototypes (left: bottom, right: top), (a) proposed antenna, (b) antenna 1, and (c) antenna 2.

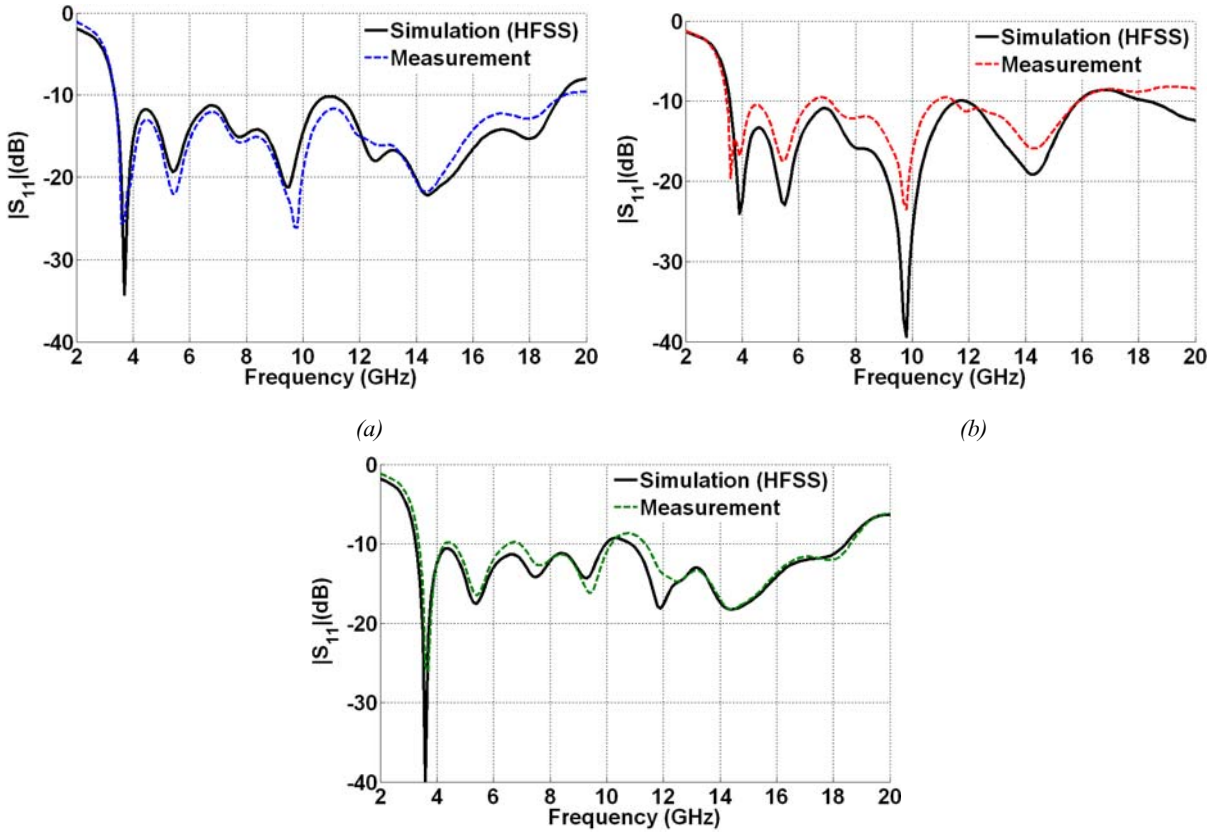

(a) *(b)*

(c)

Fig. 8. Numerical and experimental reflection coefficient curves of the antennas, (a) proposed antenna, (b) antenna 1, and (c) antenna 2.

the numerical and experimental E (x-y)-and H (y-z)-plane patterns at 4, 11, and 19 GHz are compared in Fig. 9. A good concordance between the numerical and experimental outcomes is observed. Also, Fig. 10 illustrates the simulated 3D far-field pattern of the PFABTA at 4 GHz. As shown in Figs. 9 and 10, the antenna features almost omnidirectional and bidirectional radiation

patterns in H- and E-plane, respectively. It is seen that the radiation pattern starts to deteriorate at 19 GHz because of the undesired modes at higher frequencies.

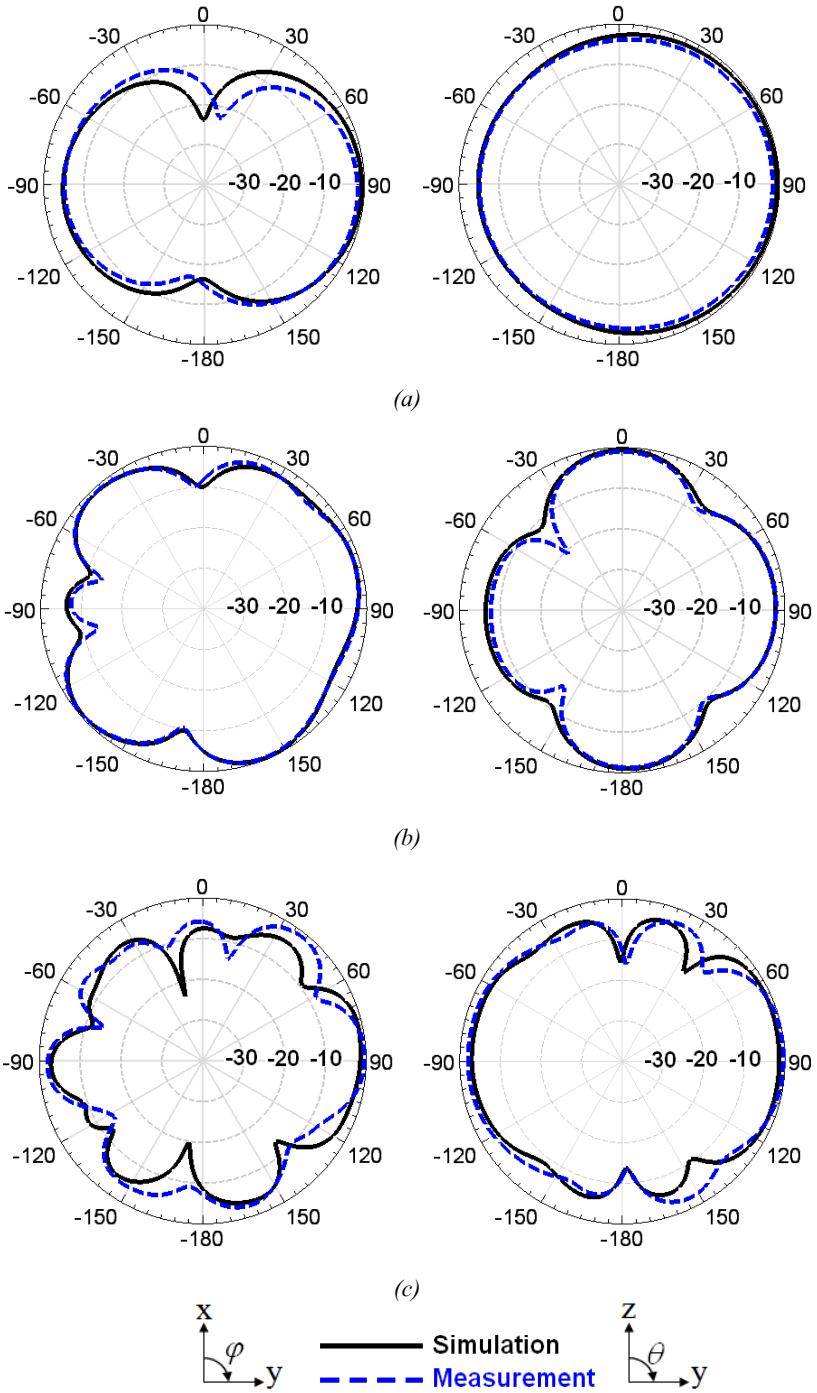

Fig. 9. Experimental and numerical far-field E (x-y)-and H (y-z)-plane patterns of the modified antenna *(left: x-y plane, right: y-z plane)* at (a) 4, (b) 11, and (c) 19 GHz.

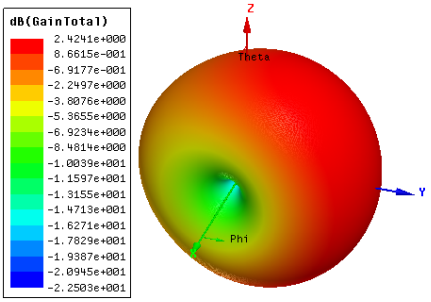

Fig. 10. Simulated 3D radiation pattern of the PFABTA at 4 GHz.

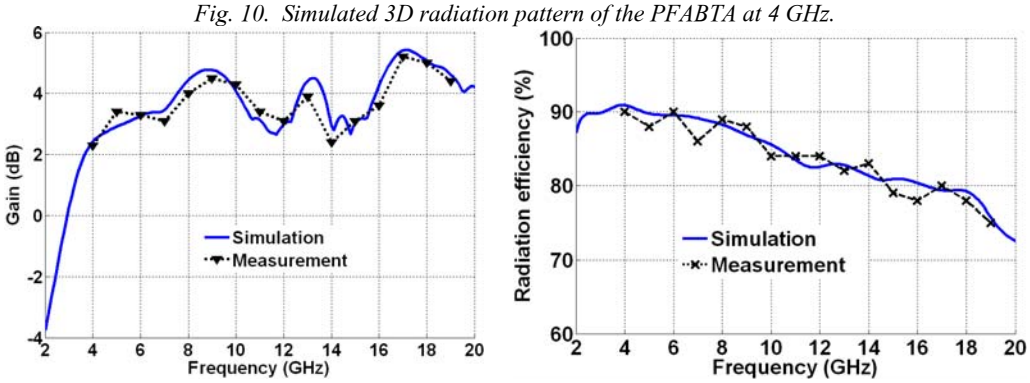

(a) *(b)*

Fig. 11. Numerical and experimental radiation characteristics of the *PFABTA* versus frequency, (a) gain, (b) radiation efficiency.

Table I. Calculated fidelity factor of the PFABTA

Angle (degrees)	*fidelity factor*	
	azimuth plane (E-plane)	*Elevation plane (H-plane)*
0	*0.88*	*0.91*
15	*0.86*	*0.88*
30	*0.85*	*0.87*
45	*0.84*	*0.85*
60	*0.82*	*0.83*
75	*0.80*	*0.81*
90	*0.78*	*0.79*

Fig. 11(a) plots the simulated and measured gain curves of the PFABTA versus frequency. The measured gain varies between 2.3 and 5.2 dB over the frequency range of 4-19 GHz and has an average value of 3.66 dB. It should be mentioned that the gain is reasonable over the working band regarding the small size of the antenna. The experimental and numerical radiation efficiency curves of the PFABTA are shown in Fig. 11(b). It is seen that the fabricated PFABTA can provide desirable efficiency of greater than 80% and 75% over the frequency bands of 4-14.5 GHz and 14.5-19 GHz, respectively. Notice that the antenna radiation efficiency is desirable considering the FR4 substrate with loss tangent of 0.02.

B. Time-domain results

In order to analyze the time-domain performance of the designed PFABTA, fidelity factor is investigated. This time-domain characteristic determines the signal distortion which an antenna adds

to its input signal. Notice that the signal distortion reduces signal-to-noise ratio and increases bit error rate in communication systems. In the last step of this work, fidelity factor is calculated by using CST Microwave Studio. By using the approach suggested in [28], the input signal is given to the antenna, and the electric field in the antenna far field is received by means of seven virtual probes. The distance between the transmitting antenna and the probes maintains at 400 mm. The fidelity factor is calculated in both E- and H-plane. In each plane, seven probes are located with the angle equal to 0°, 15°, 30°, 45°, 60°, 75°, and 90°, respectively. The calculated fidelity factor for both planes is tabulate in Table I. As shown in this table, the fidelity factor in both planes is more than 0.78, making the antenna suitable for most practical wideband applications.

To conclude, compared to recent designs reported in [22-25], the proposed antenna features broader overall bandwidth and smaller size, simultaneously. This comparison reveals the advantages of the antenna. It should be noted than the time-domain results of the antennas in [22-25], were not presented and discussed. The experimental results in frequency as well as time domain indicate that the PFABTA is a good option for broadband communication and phased array applications.

IV. CONCLUSION

A super-wideband compact printed fractal antenna with simple structure and satisfactory radiation characteristics has been presented. The proposed PFABTA possesses advantages of not only a broad bandwidth of 141 %, but also a small size of 30×34×1.2 mm^3. It can cover the C, X and Ku-bands from 3.3 to 19.1 GHz. The antenna comprises of an antipodal bow-tie with hexagonal radiators. Furthermore, Small hexagon elements are added to the sides of the antenna radiators to achieve a wide operation along with a compact size. A multi-section microstrip line with different widths is designed to match the antenna to the 50Ù SMA connector. The numerical outcomes obtained from HFSS simulator package have been verified by experimental measurements. Experimental results show that the designed PFABTA provides desirable frequency-domain characteristics such as almost omnidirectional radiation patterns, good radiation efficiency, and reasonable gain. Furthermore, to analyze the proposed antenna in time domain, fidelity factor has been presented. Compared to recent designs reported in [22-25], the proposed antenna features a wider operating bandwidth and smaller size. The proposed PFABTA is a good candidate for use in broadband communication or phased array systems due to its low profile, wide bandwidth, light weight, low cost, and ease of fabrication.

REFERENCES

[1] D. Li and J.-F. Mao, Sierpinskized koch-like sided multifractal dipole antenna, Progress In Electromagnetics Research, vol. 130, pp. 207-224, August 2012.

[2] D. Li and J.-F. Mao, Koch-like sided Sierpinski gasket multifractal dipole antenna, Progress In Electromagnetics Research, vol. 126, pp. 399-427, March 2012.

[3] M. N. A. Karim, M. K. Abd Rahim, H. A. Majid, O. B. Ayop, M. Abu, and F. Zubir, "Log periodic fractal Koch antenna for UHF band applications," Progress In Electromagnetics Research, vol. 100, pp. 201-218, 2010.

[4] M. Mahdavi, Z. Atlasbaf, and K. Forooraghi, "A very compact CPW-FED ultra-wideband circular monopole antenna,'' Microwave and Optical Technology Letters, vol. 54, no. 7, pp. 1665-1668, July 2012.

[5] R. Zaker and A. Abdipour, "Bandwidth enhancement and miniaturization of fork-shaped monopole antenna," IEEE Antennas and Wireless Propagation Letters, vol. 10, pp. 697-700, July 2011.

[6] M. Koohestani and M. Golpour, "U-shaped microstrip patch antenna with novel parasitic tuning stubs for ultra wideband applications,'' IET Microwaves Antennas and Propagation, vol. 4, no. 7, pp. 938-946, July 2010.

[7] N. Cohen, "Fractal antenna applications in wireless telecommunications,'' Professional Program Proc. of Electronics Industry Forum, pp. 43-49, 1997.

[8] J. Gianvittorio and Y. Rahmat-Samii, "Fractal element antennas: A compilation of configurations with novel characteristics,'' IEEE Antennas and Propagation Society International Symposium, Salt Lake City, UT, USA, 16-21, July 2000.

[9] C. Puente, J. Romeu, R. Pous, J. Ramis, and A. Hijazo, "Small but long Koch fractal monopole,'' Electronics Letters, vol. 34, no. 1, pp. 9-10, January 1998.

[10] R. V. Hara Prasad, Y. Purushottam, V. C. Misrak, and N. Ashok, "Microstrip fractal patch antenna for multiband communication, Electronics Letters, vol. 36, no. 14, pp. 1179-1180, July 2000.

[11] C. T. P. Song, P. S. Hall, H. Ghafouri-Shiraz, and D. Wake, "Fractal stacked monopole antenna with very wide bandwidth, Electronics Letters, vol. 35, no. 12, pp. 945-946, June 1999.

[12] C. Puente, J. Romeu, R. Pous, and A. Cardama, "On the behavior of the Sierpinski multiband fractal antenna," IEEE Transactions on Antennas and Propagation, vol. 46, no. 4, pp. 517-524, April 1998.

[13] C. Puente, "Fractal antennas," Ph.D. Dissertation at the Dept. of Signal Theory and Communications, Universitat Politkcnica de Catalunya, June 1997.

[14] Y. C. Chen, S. Y. Chen, and P.Hsu, "A compact triband bow-tie slot antenna fed by a coplanar waveguide," *IEEE Antennas and Wireless Propagation Letters, vol. 9*, pp. 1205-1208, *December 2010*.

[15] A. C. Durgun, C. A. Balanis, C. R. Birtcher, and D. R.Allee, "Design, simulation, fabrication and testing of flexible bow-tie antennas," *IEEE Transactions on Antennas and Propagation, vol. 59,* no. 12, pp. 4425-4435, *December 2011*.

[16] M. A. Antoniades and G. V. Eleftheriades, "Multiband compact printed dipole antennas using NRI-TL metamaterial loading," *IEEE Transactions on Antennas and Propagation, vol. 60, no. 12, pp.* 5613-5626, *December 2012*.

[17] D. Li and J.-f. Mao, "A koch-like sided fractal bow-tie dipole antenna," *IEEE Transactions on Antennas and Propagation, vol. 60, no. 5, pp. 2242-2251, May 2012.*

[18] J. Yang and A. Kishk," A novel low-profile compact directional ultra-wideband antenna: the self-grounded bow-tie antenna," *IEEE Transactions on Antennas and Propagation, vol. 60, no. 3, pp. 1214-1220, March 2012.*

[19] C.-C. Lin, "Compact bow-tie quasi-self-complementary antenna for UWB applications," *IEEE Antennas and Wireless Propagation Letters, vol. 11,* pp. 987–989, *August 2012*.

[20] O. Yurduseven, D. Smith, and M. Elsdon, "Printed slot loaded bow-tie antenna with super wideband radiation characteristics for imaging applications," *IEEE Transactions on Antennas and Propagation, vol. 61, no. 12, pp. 6206-6210, December 2013.*

[21] H. W. Liu, X. Zhan, S. Li, J. H. Lei, and F. Qin, "Dual-band bow-tie slot antenna fed by coplanar waveguide,'' *Electronics Letters, vol.* 50, no. 19, pp. 1338-1340, September 2014.

[22] S. Mukherjee, A. Biswas, and K. V. Srivastava, "Broadband substrate integrated waveguide cavity-backed bow-tie slot antenna," *IEEE Antennas and Wireless Propagation Letters, vol. 13, pp. 1152-1155, June 2014.*

[23] M. Jalilvand, X. Li, J. Kowalewski, and T. Zwick, "Broadband compact bow-tie antenna for 3D microwave tomography,'' *Electronics Letters, vol.* 50, no. 4, pp. 244-246, February 2014.

[24] L. Xu, L. Li, and W. Zhang, "Study and design of broadband bow-tie slot antenna fed with asymmetric CPW," *IEEE Transactions on Antennas and Propagation, vol. 63, no. 2, pp. 760-765,* February *2015.*

[25] T. Li, H. Zhai, X. Wang, L. Li, and C. Liang, "*Frequency-reconfigurable bow-tie antenna for bluetooth, WiMAX, and WLAN applications,*" *IEEE Antennas and Wireless Propagation Letters, vol. 14, pp. 171-174, 2015.*

[26] A. Dadgarpour, B. Zarghooni, B. S. Virdee, and T. A. Denidni, "Millimeter-wave high-gain SIW end-fire bow-tie antenna," *IEEE Transactions on Antennas and Propagation, vol. 63, no. 5, pp. 2337-2342, May 2015.*

[27] Y.-W. Zhong, G.-M. Yang, and L.-R. Zhong, "Gain enhancement of bow-tie antenna using fractal wideband artificial magnetic conductor ground,'' *Electronics Letters, vol.* 51, no. 4, pp. 315-317, February 2015.

[28] Q. Wu, R. Jin, J. Geng, and M. Ding, "Pulse preserving capabilities of printed circular disk monopole antennas with different grounds for the specified input signal forms," IEEE Transactions on Antennas and Propagation, Vol. 55, No. 10, pp. 2866–2873, October 2007.